International Journal of Bifurcation and Chaos, Vol. 11, No. 6 (2001) 1631–1643

CHAOTIC BURSTS AND BIFURCATION IN CHAOTIC NEURAL NETWORKS WITH RING STRUCTURE

HIROYUKI KITAJIMA
Department of Reliability-Based Information Systems Engineering, Kagawa University, Takamatsu 761-0396, Japan

TETSUYA YOSHINAGA
School of Medical Sciences, The University of Tokushima, Tokushima 770-8509, Japan

KAZUYUKI AIHARA
Department of Mathematical Engineering and Information Physics, The University of Tokyo, Tokyo 113-8656, Japan
CREST, Japan Science and Technology Corporation (JST), Saitama 332-0012, Japan

HIROSHI KAWAKAMI
Department of Electrical and Electronic Engineering, The University of Tokushima, Tokushima 770-8506, Japan

Received February 10, 2000; Revised September 15, 2000

We investigate a noninvertible map describing burst firing in a chaotic neural network model with ring structure. Since each neuron interacts with many other neurons in biological neural systems, it is important to consider global dynamics of networks composed of nonlinear neurons in order to clarify not only mechanisms of emergence of the burst firing but also its possible functional roles. We analyze parameter regions in which burst firing can be observed, and show that dynamics of strange attractors with burst firing is related to the generation of a homoclinic-like situation and vanishing of an invariant closed curve of the map.

1. Introduction

A neuron, or the fundamental element of the brain, generates various temporal patterns of spikes [Aihara & Matsumoto, 1986; Segundo *et al.*, 1995; Bargas & Galarraga, 1995].

Among such firing patterns, dynamical behavior with burst firing is considered in this paper. The burst firing is composed of bursts of neuronal spikes with nearly regular short interspike intervals, interspersed with irregularly longer interburst intervals [Selz & Mandell, 1992]. The burst firing has been found in many kinds of biological cells and its possible functions have been also discussed [Crick, 1984; Selz & Mandell, 1992; Hayashi & Ishizuka, 1992; Robinson *et al.*, 1993; Laurent & Davidowitz, 1994; Bair *et al.*, 1994; Bargas & Galarraga, 1995; Williams & Sigvardt, 1995; MacLeod & Laurent, 1996; Koch, 1999; Plenz & Kitai, 1999].

Mechanisms of generating burst firing and related rich dynamics including chaos have been intensively studied from the viewpoint of biophysical and dynamical modeling of nerve membranes by introducing slow variables to fast spiking dynamics [Carpenter & Grossberg, 1983; Chay *et al.*, 1995; Wang & Rinzel, 1995; Rinzel & Ermentrout, 1998; Izhikevich, 2000].

Since each neuron interacts with many other neurons in biological neural systems, it is important to consider global dynamics of networks composed of nonlinear neurons in order to clarify not only mechanisms of emergence of the burst firing [Han *et al.*, 1997] but also its possible functional roles.

In the paper, we examine nonlinear dynamics and bifurcations of chaotic neural networks with simple ring structure, i.e. a ring network of neurons coupled through unidirectional local interactions, in which chaotic bursts, or burst firing in strange attractors can be observed [Aihara *et al.*, 1990].

2. Model of Chaotic Neural Network with Ring Structure

We consider a noninvertible map defined by

$$T : R^n \to R^n ;\ y(t) \mapsto y(t+1) = T(y(t)) \qquad (1)$$

where $y(t) = (y_1(t), \ldots, y_n(t))^{\mathsf{T}}$ is the state vector at the discrete time t and the ith element $T_i(y(t))$ of $T(y(t)) \in R^n$ is described by

$$T_i(y(t)) = ky_i(t) + a - f(y_i(t)) + wf(y_{i+1}(t)),$$
$$\text{for } i = 1, 2, \ldots, n, \quad y_{n+1}(t) \equiv y_1(t)$$

with nonlinear function $f(y) = 1/(1 + \exp(-y/\varepsilon))$ and system parameters k, a, w and ε. The system corresponds to a chaotic neural network model [Aihara, 1989; Aihara *et al.*, 1990] with ring structure. The output $x_i(t)$ of neuron i at time t is given by

$$x_i(t) = f(y_i(t)). \qquad (2)$$

Examples of time series of the output from each neuron in strange attractors with burst firing observed in three-coupled neurons are shown in Fig. 1. We observe two types of burst firing: (i) the output of each neuron is burst firing [Fig. 1(a)] and (ii) the output of each neuron is almost "singlet" bursting [Chay *et al.*, 1995] [Fig. 1(b)], however the sum of the output of each neuron looks like burst firing [Fig. 1(c)]. In this paper, a mechanism of the production of the burst firing is investigated from the viewpoint of nonlinear network dynamics. For considering the essential mechanism of the burst firing, we treat simple networks composed of n-neurons with $n = 2, 3, 4, 6$.

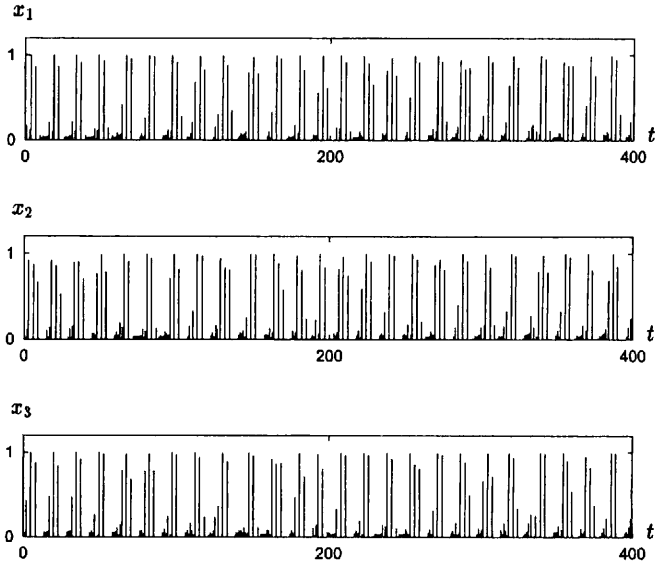

(a)

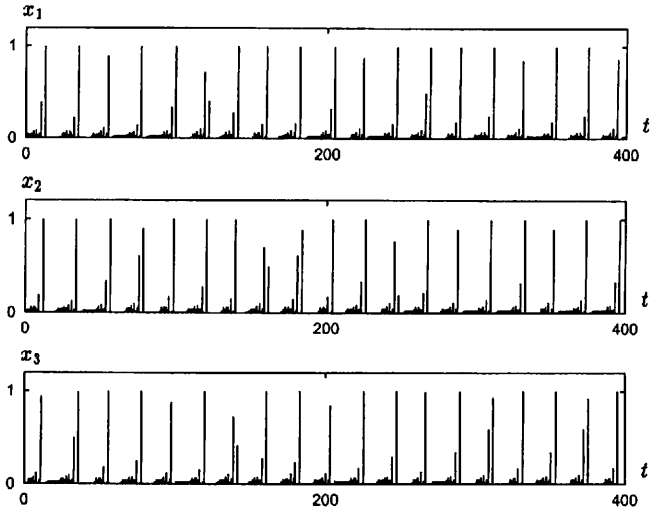

(b)

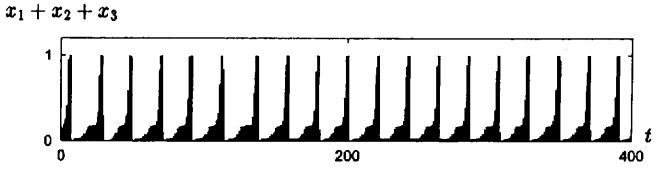

(c)

Fig. 1. Bar plots of time series of each neuron's output in strange attractors with burst firing observed in Eq. (1). We consider a response as a spike or firing if the value of the output is greater than 0.5 [Aihara *et al.*, 1990]. (a) $n = 3$, $k = 0.75$, $a = 0.02$, $w = 0.5$, $\varepsilon = 0.03$. (b) $n = 3$, $k = 0.9$, $a = 0.02$, $w = 0.5$, $\varepsilon = 0.03$. (c) The sum of x_1, x_2 and x_3. $n = 3$, $k = 0.9$, $a = 0.02$, $w = 0.5$, $\varepsilon = 0.03$.

3. Symmetric Property of The Map

Note that the map T has a symmetric property such that

$$T \circ P^j = P^j \circ T, \quad \forall j = 1, \ldots, n \tag{3}$$

where

$$P : R^n \to R^n;\ y(t) \mapsto \begin{pmatrix} 0 & 1 & 0 & \cdots & 0 \\ 0 & 0 & 1 & \cdots & 0 \\ & & \cdots & & \\ 1 & 0 & 0 & \cdots & 0 \end{pmatrix} y(t).$$

The set of transformations $G = \{I, P, P^2, \ldots, P^{n-1}\}$, where I denotes the identity transformation, is a cyclic group of order n, then the map T is G-equivariant. If there exists an invariant subspace

$$\Pi_i : \{y | P^i y = y\}$$

for some $i = 1, 2, \ldots, n-1$, then we have a subsystem that behaves in the subspace. We see that the n-coupled system has a subsystem of m-coupled systems, where m is any factor of the integer n.

The existence of an m-periodic point u of T, satisfying $P^j(u) = T(u)$, namely a P^j-symmetric m-periodic point, plays an important role on the generation of burst firing. We show periodic points and strange attractors representing burst firing in the state space by using the following projection from R^n, $n \geq 3$, to the plane R^2:

$$Q : R^n \to R^2$$

$$y \mapsto \sqrt{\frac{2}{n}} \begin{pmatrix} 1 & \cos\left(2\pi\frac{1}{n}\right) & \cos\left(2\pi\frac{2}{n}\right) & \cdots \\ 0 & \sin\left(2\pi\frac{1}{n}\right) & \sin\left(2\pi\frac{2}{n}\right) & \cdots \end{pmatrix} y. \tag{4}$$

4. Method for Calculating Local Bifurcations

Before showing results, we summarize methods and notations about analysis of periodic points in the map T. The point y^* satisfying

$$y^* - T^m(y^*) = 0 \tag{5}$$

becomes a fixed ($m = 1$) or an m-periodic ($m > 1$) point of T. Let $y^* \in R^n$ be such a periodic point of T. Then the characteristic equation of the periodic point y^* is defined by

$$\det(\mu I - DT^m(y^*)) = 0 \tag{6}$$

where I is the $n \times n$ identity matrix, and DT^m denote the derivative of T^m. We call y^* is hyperbolic, if all the absolute values of the eigenvalues of T^m are different from unity. The symbol ${}_kD^m$ (resp. ${}_kI^m$) denotes a hyperbolic periodic point such that D (resp. I) indicates a type with even (resp. odd) number of characteristic multipliers on the real axis $(-\infty, -1)$, k indicates the number of characteristic multiplier outside the unit circle in the complex plane, and m indicates an m-periodic point.

A local bifurcation occurs when the topological type of a periodic point is changed by the variation of the system parameter values. In the following section we will observe generic codimension-one bifurcations of tangent, period-doubling and Neimark–Sacker bifurcations. These bifurcations are observed when the hyperbolicity is destroyed due to the critical distribution of characteristic multipliers μ such that $\mu = +1$ for the tangent bifurcation, $\mu = -1$ for the period-doubling bifurcation, and $\mu = e^{j\theta}$ for the Neimark–Sacker bifurcation, where $j = \sqrt{-1}$. To calculate local bifurcations, we use the method proposed by Kawakami [1984]. Namely the fixed or periodic point equation of Eq. (5) and the bifurcation condition of Eq. (6) are simultaneously solved by Newton's method.

In the bifurcation diagram, the tangent, period-doubling and Neimark–Sacker bifurcation sets of m-periodic points are indicated by thick, fine and dotted curves with symbols G_ℓ^m, I_ℓ^m and NS_ℓ^m, respectively, where ℓ is the index number to distinguish the same bifurcation type.

5. Numerical Results

5.1. *Bifurcation of uncoupled system*

First, we show some results of an uncoupled system of a single chaotic neuron [$n = 1$ and $w = 0$ in Eq. (1)] [Aihara *et al.*, 1990], i.e.

$$y_1(t+1) = ky_1(t) + a - f(y_1(t)). \tag{7}$$

Figure 2 indicates a bifurcation diagram of the chaotic neuron in the parameter plane (a, k) with

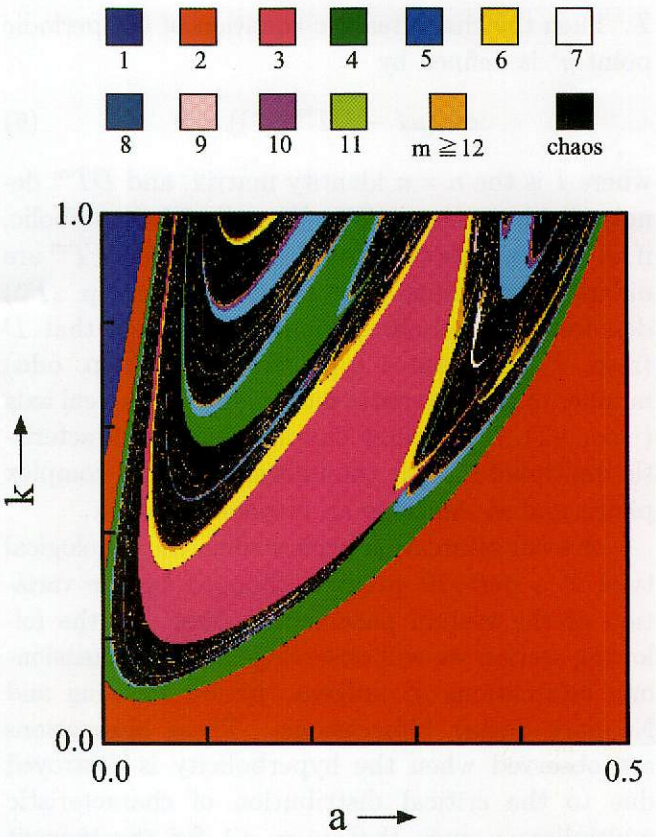

Fig. 2. Bifurcation diagram of Eq. (7) with $\varepsilon = 0.02$ in the parameter plane (a, k). In each colored region denoted by m, we can observe an m-periodic point. The periods are defined by the upper colored squares. The black color corresponds to chaotic behavior in the sense that periodicity cannot be observed with the resolution of 10^{-8} in 10,000 iterated points.

$\varepsilon = 0.02$, showing that various kinds of periodic and chaotic solutions can be obtained in this neuron model. This bifurcation diagram as a coarse view is for visualizing long-term behavior of the system with global variation of the system parameters and shows transitions of attractors emanating from a certain initial value. To investigate exact formulae of bifurcations of periodic points, we also examined the bifurcation structure with the method stated in the previous section. From both kinds of bifurcation diagrams, we see that periodic solutions are generated by either tangent or period-doubling bifurcations and that chaotic solutions are generated by successive period-doubling bifurcations. Figure 3 is an enlargement of a part of Fig. 2. In some parameter regions, periodic solutions coexist due to the existence of tangent bifurcations and their cusp points; this is a property peculiar to bimodal maps [Fraser & Kapral, 1982; Aihara *et al.*, 1990].

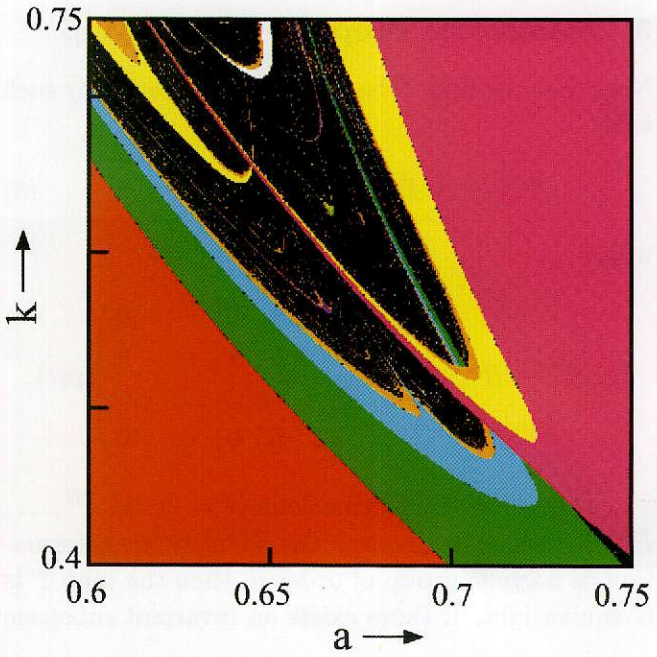

Fig. 3. Enlarged diagram of a part of Fig. 2.

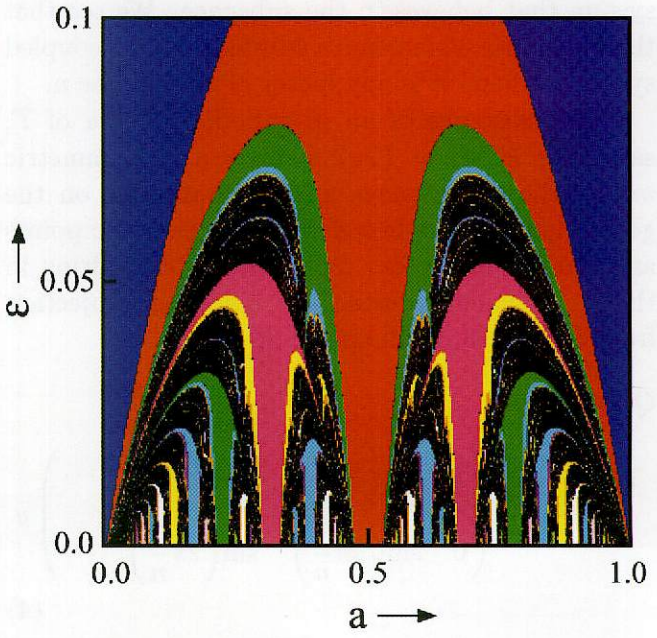

Fig. 4. Bifurcation diagram of Eq. (7) with $k = 0.9$ in the parameter plane (a, ε). The meaning of colors is the same as Fig. 2.

Figure 4 indicates a bifurcation diagram in the parameter plane (a, ε) with $k = 0.9$.

5.2. *Bifurcation of one-dimensional subsystem for coupling system*

Let us consider one-dimensional map of Eq. (1)

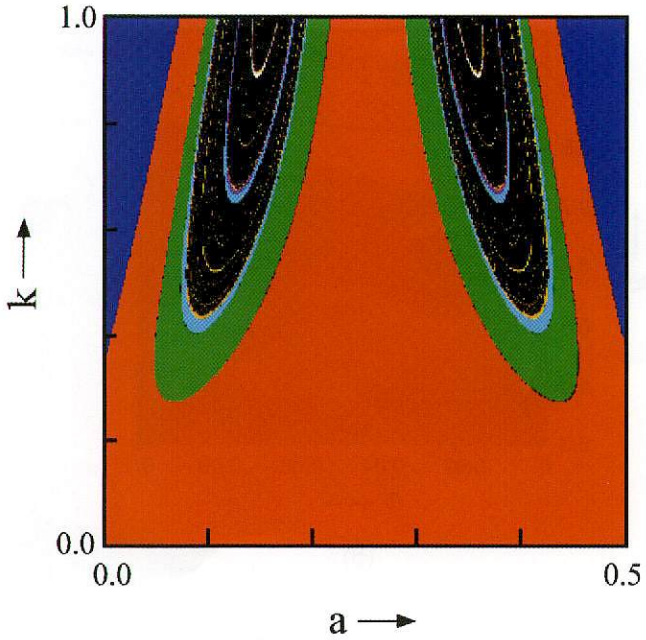

Fig. 5. Bifurcation diagram of Eq. (8) with $w = 0.5$ and $\varepsilon = 0.03$ in the parameter plane (a, k). The meaning of colors is the same as Fig. 2.

with $n = 1$, i.e.

$$y_1(t+1) = ky_1(t) + a - (1-w)f(y_1(t)). \qquad (8)$$

Recall that the n-coupled system of Eq. (1) has a subsystem of m-coupled systems, where m is any factor of the integer n. Therefore the one-dimensional system is a subsystem for the original system of Eq. (1) with arbitrary number of coupled neurons.

In the following, we fix the values of the system parameters as $w = 0.5$ and $\varepsilon = 0.03$, and consider bifurcations in parameter plane (a, k). The bifurcation diagram for attractors globally observed in the system is shown in Fig. 5. Comparison between Figs. 2 (in the case of $w = 0$) and 5 (in the case of $w = 0.5$) shows that the bifurcation diagrams have similarity, but the complexity changes due to the variation of the value of w. Figure 6 obtained by Kawakami's method [1984] shows a bifurcation diagram of a fixed point and periodic points. The single neuron dynamics produces strange attractors after accumulation of successive period-doubling bifurcations in the parameter region as shown in Fig. 6. The regions in which stable fixed, 2-periodic, 4-periodic and 8-periodic points exist are denoted by the shading ■, ■, ■ and ■, respectively.

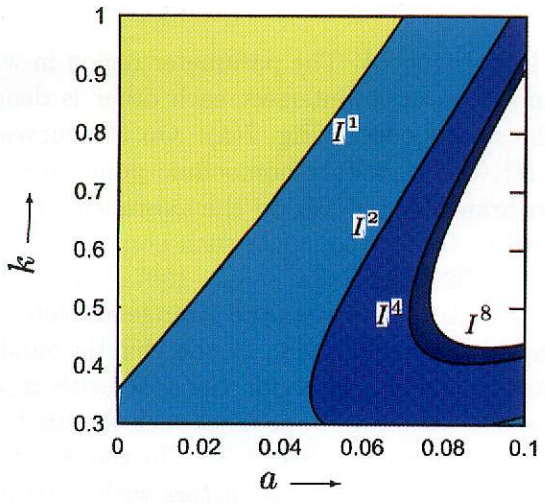

Fig. 6. Period-doubling bifurcations observed in Eq. (8).

5.3. *Results of coupled systems*

In this section we consider chaotic neural networks, Eq. (1), with ring structure composed of n neurons with $n = 2$, 3, 4 and 6. Each figure shown in Fig. 7 obtained by Kawakami's method [1984] represents a bifurcation diagram with local and global bifurcations. Parameter regions in which stable fixed and periodic points exist are denoted by the shading ■, ■ and ■. In each bifurcation diagram, the parameter region denoted by ■ shows existence of homoclinic-like structure which may generate strange attractors with burst firing, namely chaotic bursts. Detailed explanation of the homoclinic-like structure will be given in Sec. 5.3.2. The strange attractors observed at the parameter value labeled by p in Fig. 7 have characteristic forms in the state space as shown in Fig. 8. For $n \geq 3$, the n-dimensional state space is projected by Eq. (4) to the plane $(u, v)^{\mathsf{T}} = Qy$.

Now, we consider a mechanism of the generation of the strange attractors with burst firing. Each of Figs. 9(a)–9(d) shows an α-branch or an unstable set of a saddle fixed or periodic point, coexisting with a strange attractor shown in Fig. 8, which is obtained as a steady state of the simulation emanating from an initial condition except for the α-branch. The α-branch of Fig. 9 was numerically calculated by the method in [You *et al.*, 1991]. It should be noted that self-intersections of the α-branch are possible, because Eq. (1) is a noninvertible map [Millerioux & Mira, 1997]. We see that the strange attractor coexists with the α-branch as shown in Figs. 8 and 9. The emergence of the strange attractor is related to vanishing of an invariant closed curve of T^n after generating a

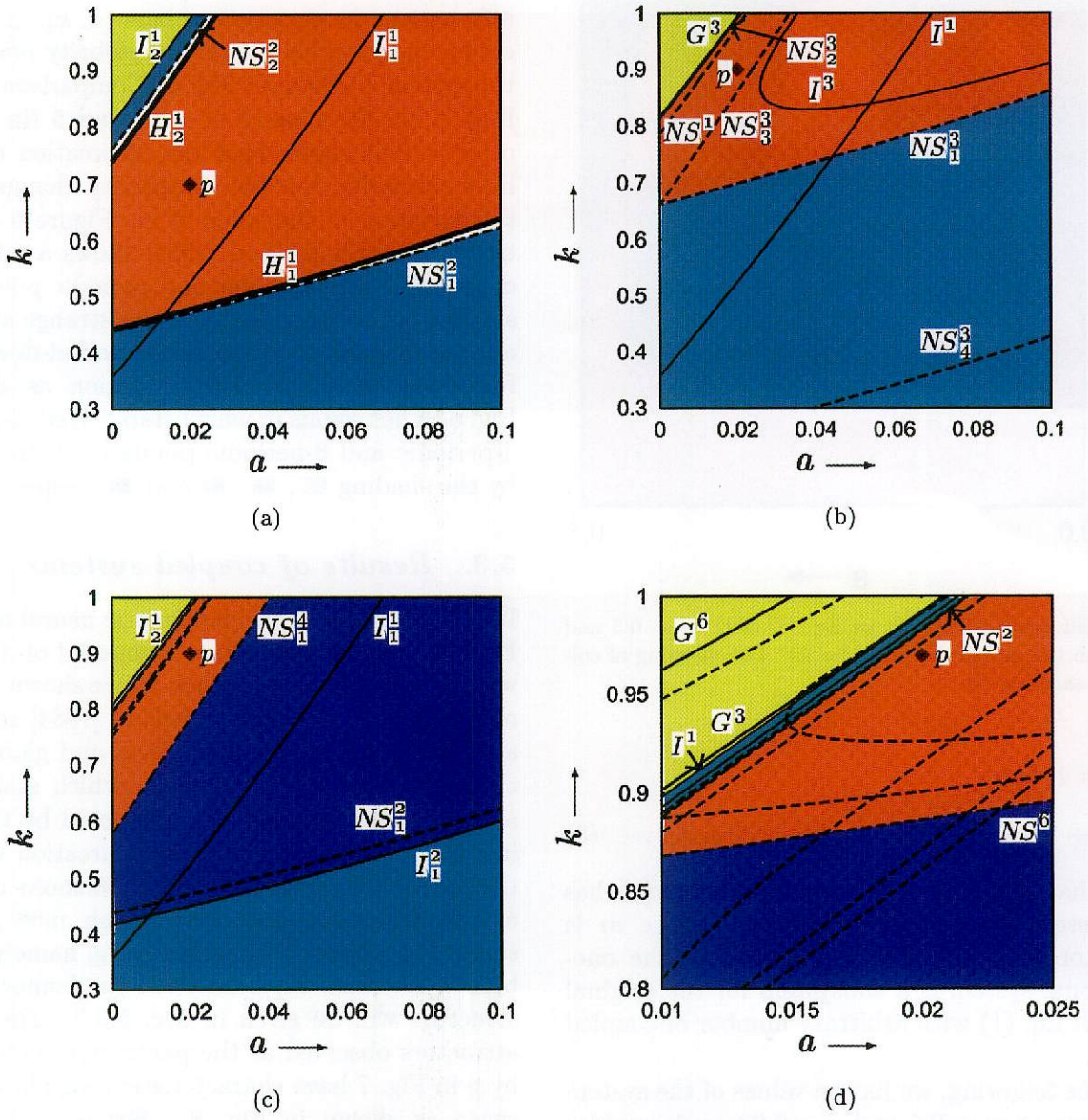

Fig. 7. Bifurcation diagrams observed in Eq. (1) with $n = 2$, 3, 4 and 6. On the curves H_1^1 and H_2^1, there exists a homoclinic point such that the α-branch is tangent to the ω-branch. (a) $n = 2$, (b) $n = 3$, (c) $n = 4$, (d) $n = 6$.

homoclinic-like situation, as studied below where dynamics of n-coupled neurons with $n = 2$, 3, 4 and 6 are investigated.

5.3.1. *The case of* $n = 2$

The stable fixed point, which exists in the region in Fig. 7(a), changes its stability to the type ${}_1I^1$ by passing through the period-doubling bifurcation curve I_2^1, whose eigenvector with respect to the unstable characteristic multiplier has the direction $(\pm 1, \mp 1)^{\mathrm{T}}$ [Judd *et al.*, 1991]; see the α-branch of the fixed point ${}_1I^1$shown in Fig. 9(a). Because the ω-branch is on the line $y_1 = y_2$, a homoclinic situation is constructed. The parameter region in which α- and ω-branches intersect each other is denoted by the shading in Fig. 7(a). On the curves H_1^1 and H_2^1, there exists a homoclinic point such that the α-branch is tangent to the ω-branch. The numerical method to calculate such homoclinic points is shown in [Yoshinaga *et al.*, 1997]. The homoclinic structure generates the strange attractor representing the burst firing, or the chaotic bursts as demonstrated in Fig. 1 for the case with $n = 3$. Dynamical structure to produce such chaotic bursts will be considered in Sec. 5.3.2. In the shaded region , similar strange attractors with burst firing can be observed.

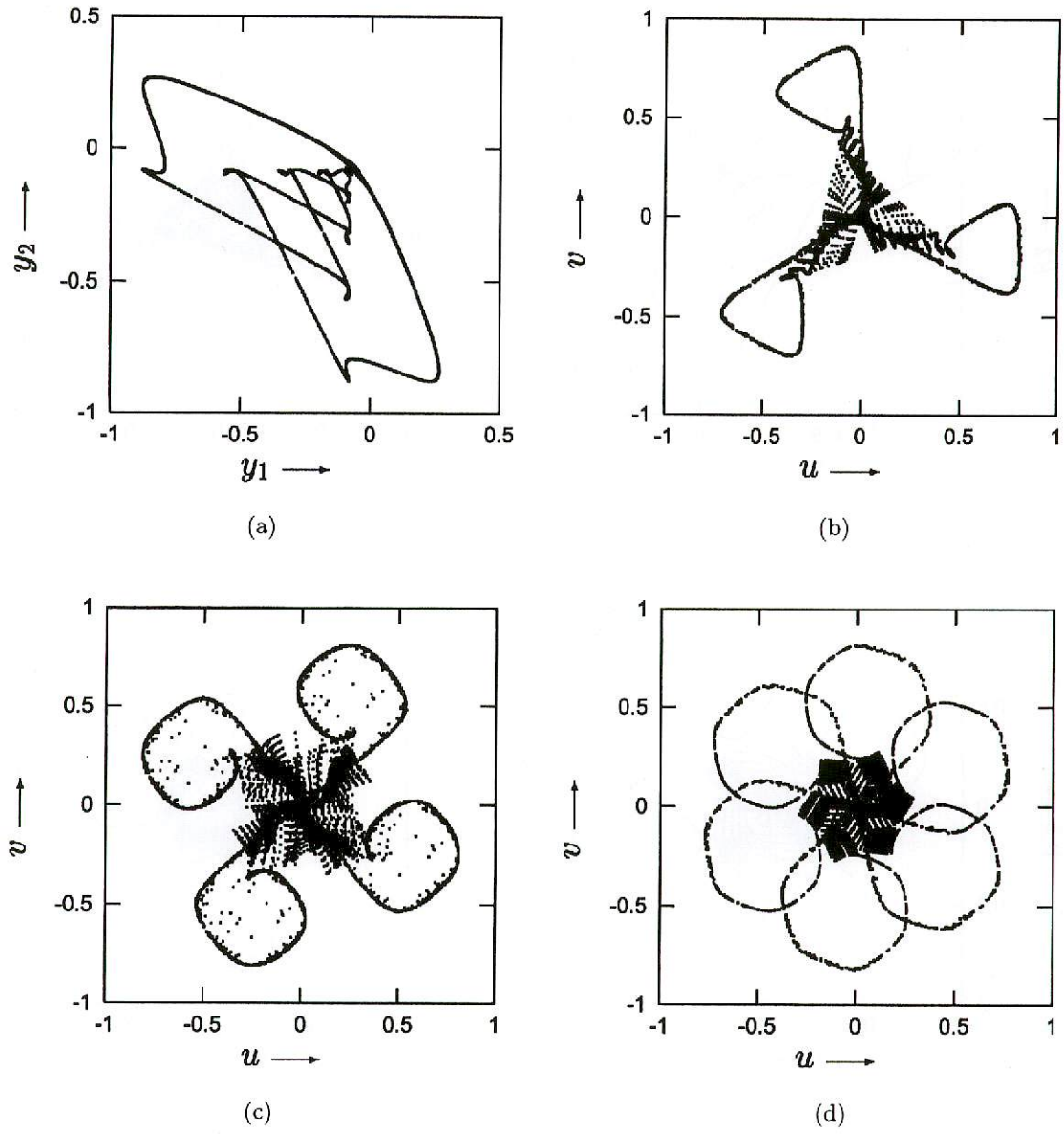

Fig. 8. Strange attractors observed in Eq. (1) at the parameter values marked by p in Figs. 7(a)–7(d). (a) $n = 2$, $a = 0.02$, $k = 0.7$. (b) $n = 3$, $a = 0.02$, $k = 0.9$. (c) $n = 4$, $a = 0.02$, $k = 0.9$. (d) $n = 6$, $a = 0.02$, $k = 0.97$.

5.3.2. *The case of* $n = 3$

For the three-coupled neurons, 3-periodic points are related to the occurrence of chaotic bursts. Figure 7(b) shows bifurcations of fixed and P^2-symmetric 3-periodic points. In regions ■ and ■, stable fixed and P^2-symmetric 3-periodic points exist, respectively. At the point labeled by p in Fig. 7(b), there is a 3-periodic point ${}_1D^3$ generated by the tangent bifurcation G^3. The α-branch of the 3-periodic point ${}_1D^3$ is shown in Fig. 9(b). The α-branch returns again around the 3-periodic point ${}_1D^3$, then a homoclinic-like situation is constructed. Indeed, at the same parameter values, we see chaotic bursts around the α-branch as shown in Fig. 8(b). To understand the mechanism of the generation of the chaotic bursts, the transition of the α-branch of the 3-periodic point ${}_1D^3$ is shown in Fig. 10. At $k = 0.663$ [Fig. 10(a)], the α-branch of the 3-periodic point ${}_1D^3$ goes to the stable P^2-symmetric 3-periodic point ${}_0D^3$. The 3-periodic point ${}_1D^3$ is two-dimensionally stable, and near the 3-periodic point ${}_1D^3$ there exists two-dimensionally unstable fixed point ${}_2D^1$. By increasing the value of k the stable P^2-symmetric 3-periodic point ${}_0D^3$ becomes two-dimensionally unstable (${}_2D^3$) by a Neimark–Saker bifurcation in the set NS_1^3 of Fig. 7(b) and generates an invariant

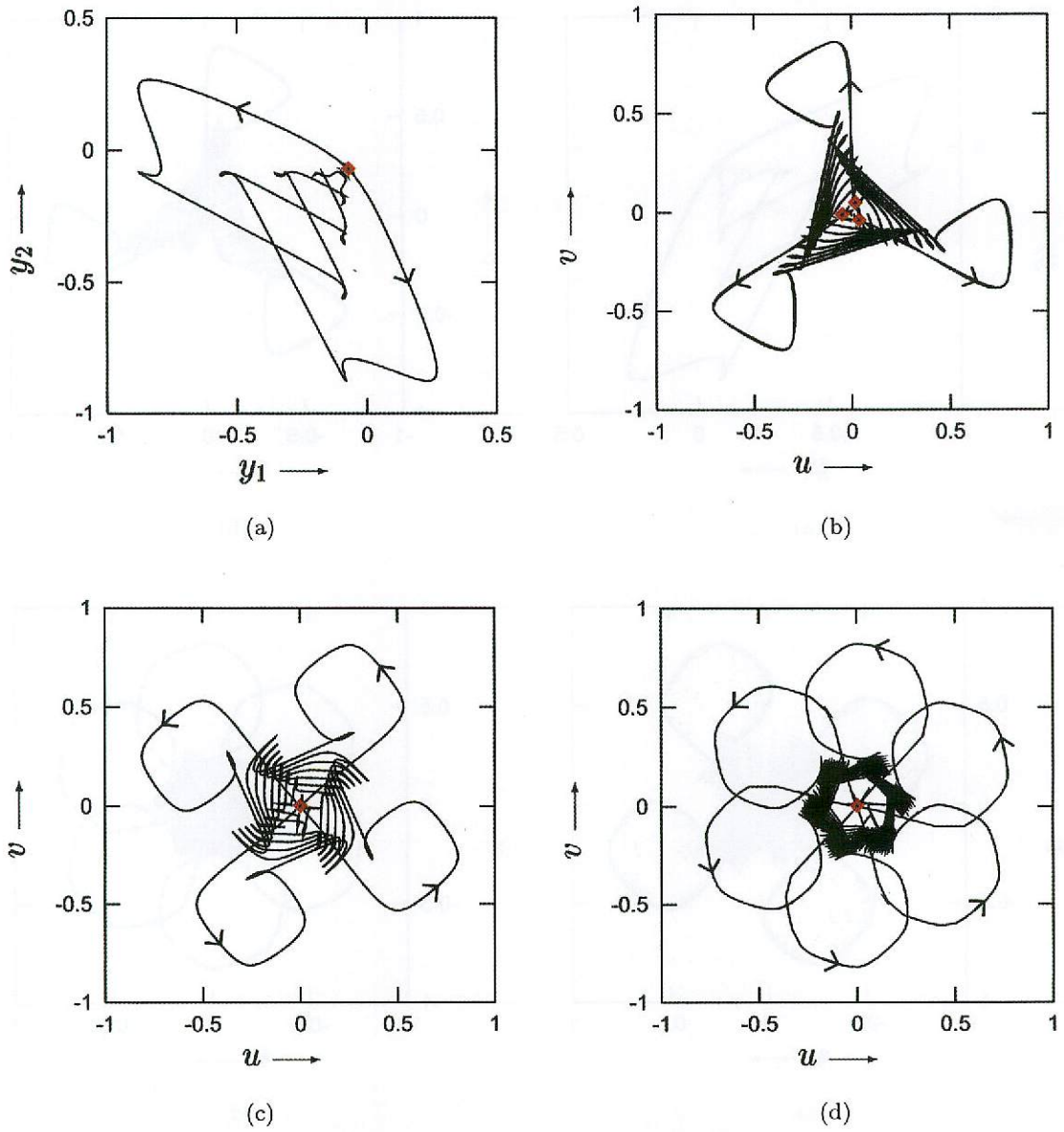

Fig. 9. The α-branch of (a) ${}_1I^1$, (b) ${}_1D^3$, (c) ${}_3I^2$ and (d) ${}_3I^3$ of Eq. (1) with $n = 2$, 3, 4 and 6, respectively. (a) $n = 2$, (b) $n = 3$, (c) $n = 4$, (d) $n = 6$.

closed curve of T^3 [Fig. 10(b)]. The invariant closed curve turns into an annular strange attractor [Mira, 1987] and the chaotic bursts appears due to merging of three disconnected annular chaotic areas by further increasing of k [Fig. 10(c)]. A schematic diagram of the homoclinic-like structure is shown in Fig. 11. The parameter region with the homoclinic-like structure is shaded by ■ in Fig. 7(b). We can observe chaotic bursts widely in the region ■. To examine the bursting property, we calculate the coefficient of variation (C_v) of the interspike intervals (ISI) which is defined by the standard deviation divided by the mean of the ISI distribution. Figure 12 shows the values of C_v for output x_1 of neuron 1 [Fig. 12(a)] and the sum of outputs x_1, x_2 and x_3 [Fig. 12(b)] in the same parameter plane as in Fig. 7(b). In the shaded region ■ of Figs. 12(a) and 12(b), we observe the chaotic bursts as shown in Figs. 1(a) and 1(c), respectively. We see that the regions in which an attractor with $C_v \geq 0.4$ exists are included in the region ■ in Fig. 7(b). We also analyze an excitation number r which is defined as follows:

(1) For output of a single neuron, r is defined by the number of spikes divided by that of iterations.

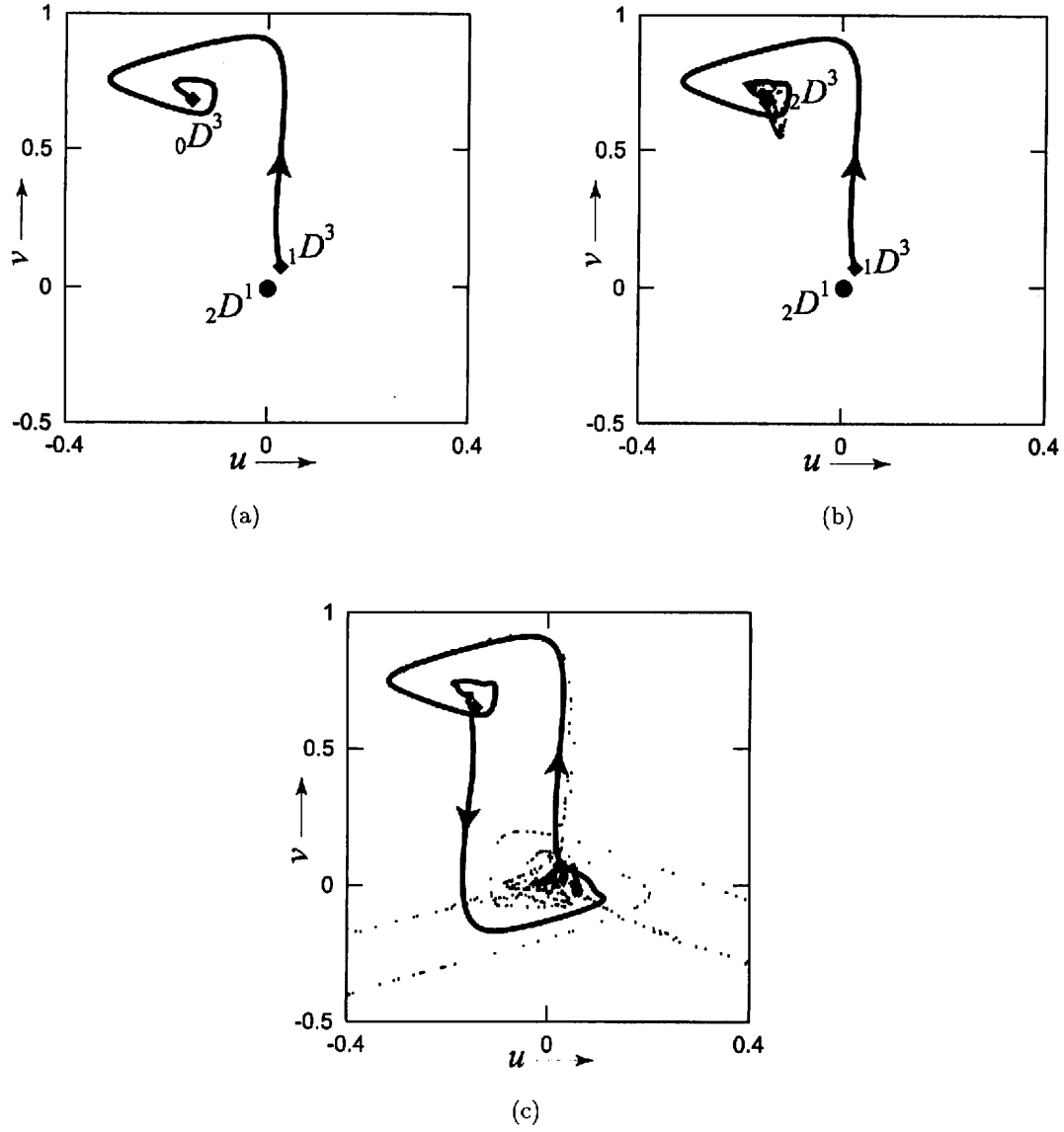

Fig. 10. Transition of the α-branch in relation to chaotic bursts of three-coupled neurons with $a = 0$ and (a) $k = 0.663$, (b) $k = 0.664$, (c) $k = 0.67$.

(2) For behavior of a network, r is defined by the number of points outside of the disk satisfying $d < 0.5$, where d is an Euclidean distance from the origin in (u, v)-plane, divided by the number of iterations.

Figure 13 shows the value of r in the same parameter plane as in Fig. 7(b). We see that the regions in which an attractor with $r \in [0.1, 0.9]$ exists are included in the region ■ in Fig. 7(b), similarly to Fig. 12.

5.3.3. *The case of* $n = 4$

The periodic point related to the occurrence of the chaotic bursts is a P-symmetric 2-periodic point $_3I^2$. The α-branch of the periodic point $_3I^2$ at the parameter values marked by p in Fig. 7(c) is shown in Fig. 9(c). The curve NS_1^4 in Fig. 7(c) denotes a Neimark–Sacker bifurcation of a stable 4-periodic point which exists in the parameter region ■ and is generated by the period-doubling bifurcation I_1^2 of a 2-periodic point. The generation of the chaotic bursts is related to vanishing of an invariant closed curve of T^4, which is caused by NS_1^4, as the similar mechanism for the case of $n = 3$. The region of the parameter values for the existence of the homoclinic-like structure in which the characteristic multipliers of a fixed point and periodic points satisfy the condition of Fig. 11, is shaded

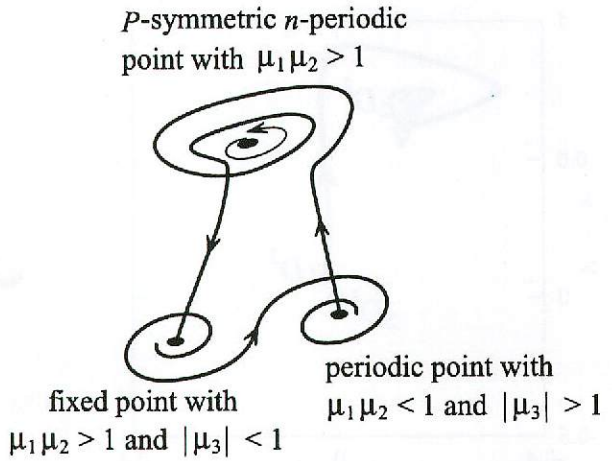

Fig. 11. A schematic diagram of homoclinic-like structure. μ_1 and μ_2 are complex conjugate characteristic multipliers and μ_3 is a real characteristic multiplier.

by ■ in Fig. 7(c). In most part of the region ■, we can observe the chaotic bursts.

5.3.4. *The case of* $n = 6$

The six-coupled neuron system has three subsystems: single, two-coupled and three-coupled neurons. Therefore the bifurcations include those for each subsystem. The periodic point related to the occurrence of the chaotic bursts is a P^2-symmetric 3-periodic point ${}_3I^3$. The α-branch of the periodic point ${}_3I^3$ at the parameter values marked by p in Fig. 7(d) is shown in Fig. 9(d). Considering the Neimark–Sacker bifurcation NS^6 in Fig. 7(d), which generates an invariant closed curve of T^6, the region of the parameter values for the existence of the homoclinic-like structure in which the characteristic multipliers of a fixed point and periodic points satisfy the condition of Fig. 11, is shaded by ■ in Fig. 7(d). The chaotic bursts are widely observed in the region ■.

6. Discussion

We have shown that chaotic neural networks with ring structure can generate strange attractors with burst firing. The network is composed of nonlinear neuron models with their own chaotic dynamics in the single neuron level [Aihara *et al.*, 1990; Aihara,

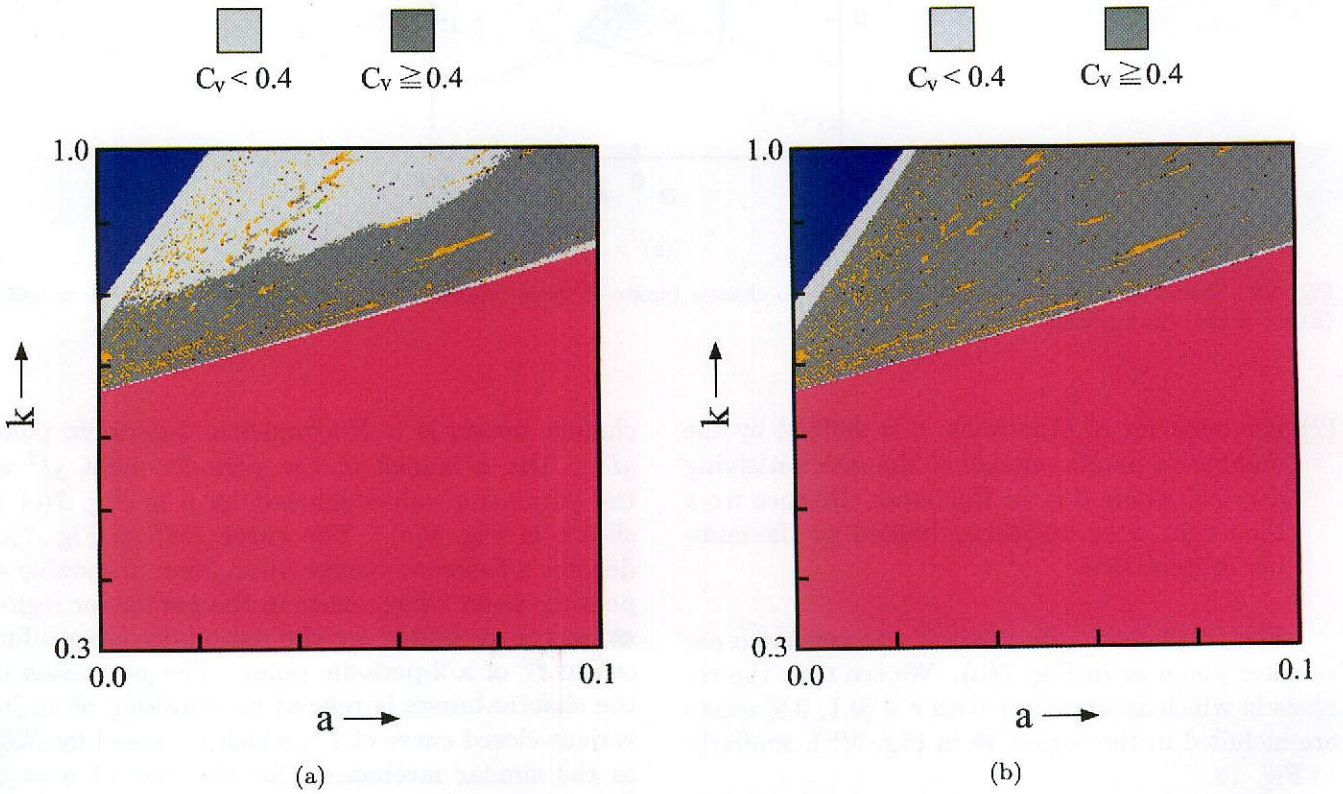

Fig. 12. Coefficient of variation (C_v) of interspike intervals (ISI) observed in three-coupled neurons. The dark gray color corresponds to a nonperiodic attractor with $C_v \geq 0.4$. The meaning of colors except the gray colors is the same as Fig. 2. We see window regions of periodic points in the gray color region. (a) C_v of ISI for output x_1 of neuron 1. (b) C_v of ISI for the sum of x_1, x_2 and x_3.

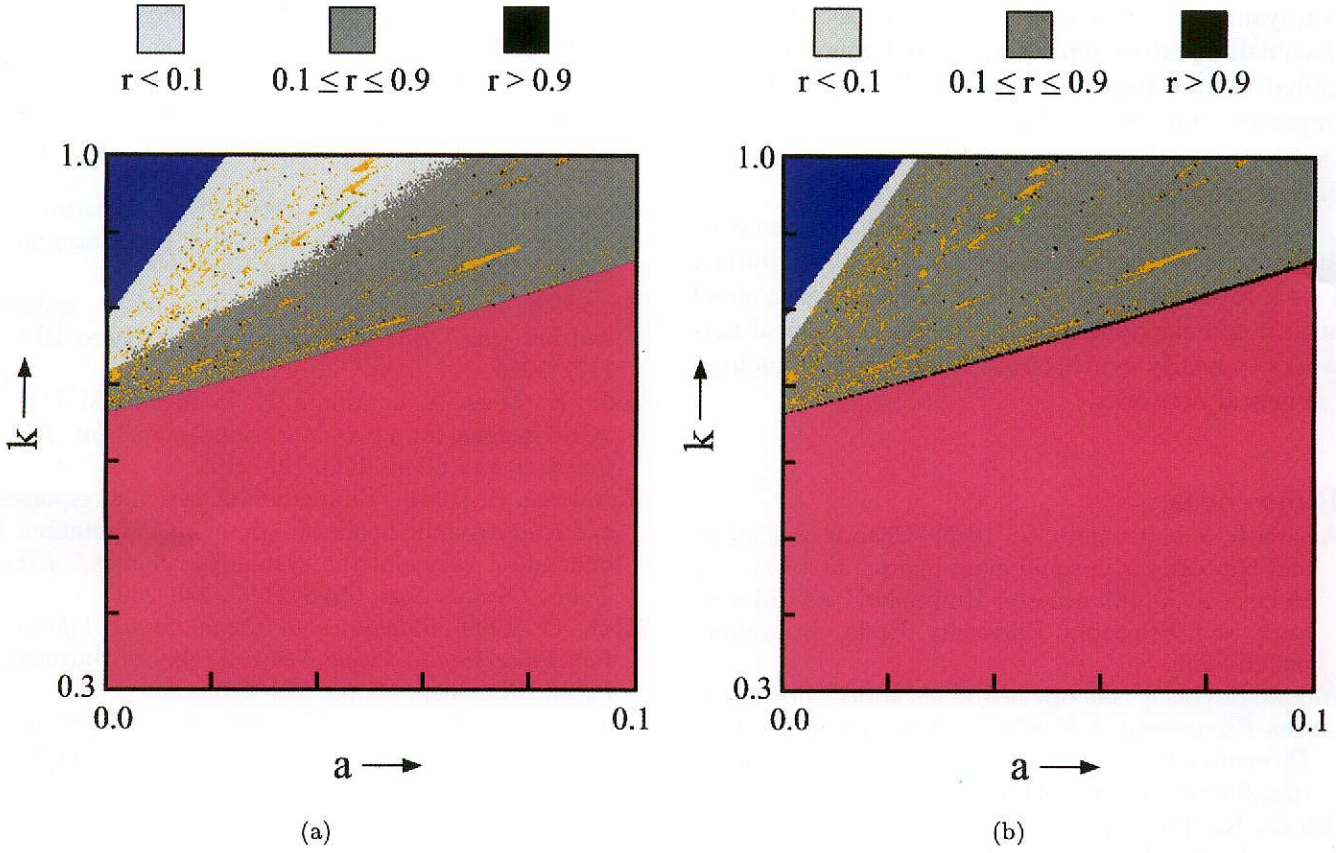

Fig. 13. Excitation number r of attractors in three-coupled neurons. The dark gray color corresponds to a nonperiodic attractor with $r \in [0.1, 0.9]$. The meaning of colors except the gray colors is the same as Fig. 2. We see window regions of periodic points in the gray color region. (a) r for output x_1 of neuron 1. (b) r for the sum of x_1, x_2 and x_3.

1990]. Therefore, the burst firing is a collective behavior in the network level organized through unidirectional local interactions between neurons, peculiar to the ring structure. It should be noted that nearly synchronous burst firing similar to chaotic bursts demonstrated in this paper is observed in neural networks of central pattern generators composed of a small number of neurons of which the dynamics is chaotic when isolated [Szücs *et al.*, 2000]. However, since the network model in this paper is highly simplified as a model of biological neural networks, it is a future problem to extend the model by considering more realistic properties like time delays [Campbell *et al.*, 1999], mutual interaction rather than unidirectional interactions peculiar to the ring structure and contribution of inhibitory neurons to synchronous burst firing [MacLeod & Laurent, 1996; Plenz & Kitai, 1999].

We have observed two types of chaotic bursts in the chaotic neural network with ring structure; one is burst firing of each single neuron as usually observed in biological neurons [Fig. 1(a)] and the other is burst firing as superposition of output of each neuron [Fig. 1(c)]. It should be noted that an effect of the superposed burst firing to a postsynaptic neuron is similar to one of usual burst firing of a single neuron if most constituent neurons of the ring network have synaptic connections to a common postsynaptic neuron with almost same delays.

7. Conclusions

We have investigated a mechanism of the generation of the burst firing observed in chaotic neural networks with the ring structure. The main results obtained from the analysis are summarized as follows: (1) We have found that the chaotic bursts are related to α-branches of P^j-symmetric periodic points; and (2) the strange attractor appears when an invariant closed curve of T^n, which is generated by a Neimark–Sacker bifurcation of an n-periodic point, vanishes after generating a homoclinic-like situation due to the change of the system parameter values. Critical curves (or manifolds) [Mira &

Narayaninsamy, 1993], i.e. images of sets that the Jacobian equal to zero, play a fundamental role in global bifurcations of noninvertible maps. It is an important future problem to investigate the relation between the homoclinic-like situation and the critical manifold.

It is conjectured that the coupled neurons with any number of coupling can produce chaotic bursts. It is a future work to consider possible relations of such nonlinear dynamics of the chaotic neural networks to nearly synchronous burst firing of biological neural networks.

References

Aihara, K. & Matsumoto, G. [1986] "Chaotic oscillations and bifurcations in squid giant axons," in *Chaos*, ed. Holden, A. V. (Manchester University Press, Manchester and Princeton University Press, Princeton), pp. 257–269.

Aihara, K. [1990] "Chaotic neural networks," in *Bifurcation Phenomena in Nonlinear Systems and Theory of Dynamical Systems*, ed. Kawakami, H. (World Scientific, Singapore), pp. 143–161.

Aihara, K., Takabe, T. & Toyoda, M. [1990] "Chaotic neural networks," *Phys. Lett.* **A**(144), 333–340.

Arshavsky, Y. I., Deliagina, T. G., Orlovsky, G. N. & Panchin, Y. V. [1998] "Control of feeding movements in the freshwater snail Planorbis corneus," *Exp. Brain Res.* **70**, 323–331.

Bair, W., Koch, C., Newsome, W. & Britten, K. [1994] "Power spectrum analysis of bursting cells in area MT in the behaving monkey," *J. Neurosci.* **14**(5), 2870–2892.

Bargas, J. & Galarraga, E. [1995] "Ion channels: Keys to neuronal specialization," in *The Handbook of Brain Theory and Neural Networks*, ed. Arbib, M. A. (The MIT Press, Cambridge), pp. 496–501.

Campbell, S. A., Ruan, S. & Wei, J. [1999] "Qualitative analysis of a neural network model with multiple time delays," *Int. J. Bifurcation and Chaos* **9**(8), 1585–1595.

Carpenter, G. A. & Grossberg, S. [1983] "Dynamic models of neural systems: Propagated signals, photoreceptor transduction, and circadian rhythms," in *Oscillations in Mathematical Biology*, ed. Hodgson, J. P. E. (Springer-Verlag, Berlin), pp. 102–196.

Chay, T. R., Fan, Y. S. & Lee, Y. S. [1995] "Bursting, spiking, chaos, fractals, and universality in biological rhythms," *Int. J. Bifurcation and Chaos* **5**(3), 595–635.

Crick, F. C. [1984] "The function of the thalamic reticular complex: The searchlight hypothesis," *Proc. Natl. Acad. Sci. USA* **81**, 4586–4590.

Fraser, S. & Kapral, R. [1982] "Analysis of flow hysteresis by a one-dimensional map," *Phys. Rev.* **A25**, 3223–3233.

Han, S. K., Park, S. H., Yim, T. G., Kim, S. & Kim, S. [1997] "Chaotic bursting behavior of coupled neural oscillators," *Int. J. Bifurcation and Chaos* **7**(4), 877–888.

Hayashi, H. & Ishizuka, S. [1992] "Chaotic nature of bursting discharges in the Onchidium pacemaker neuron," *J. Theor. Biol.* **156**, 269–291.

Izhikevich, E. M. [2000] "Neural excitability, spiking and bursting," *Int. J. Bifurcation and Chaos* **10**(6), 1171–1266.

Judd, K., Mees, A. I., Aihara, K. & Toyoda, M. [1991] "Grid imaging for a two-dimensional map," *Int. J. Bifurcation and Chaos* **1**(1), 197–210.

Kawakami, H. [1984] "Bifurcation of periodic responses in forced dynamic nonlinear circuits: Computation of bifurcation values of the system parameters," *IEEE Trans. Circuits Syst.* **CAS-31**(3), 246–260.

Koch, C. [1999] *Biophysics of Computation: Information Processing in Single Neurons* (Oxford University Press, NY), Chap. 16, pp. 374–380.

Laurent, G. & Davidowitz, H. [1994] "Encoding of olfactory information with oscillating neural assemblies," *Science* **265**, 1872–1875.

MacLeod, K. & Laurent, G. [1996] "Distinct mechanisms for synchronization and temporal patterning of odor-encoding neural assemblies," *Science* **274**, 976–979.

Millerioux, G. & Mira, C. [1997] "Homoclinic and heteroclinic situations specific to two-dimensional noninvertible maps," *Int. J. Bifurcation and Chaos* **7**(1), 39–70.

Mira, C. [1987] *Chaotic Dynamics* (World Scientific, Singapore).

Mira, C. & Narayaninsamy, T. [1993] "On behaviors of two-dimensional endomorphisms: Role of the critical curves," *Int. J. Bifurcation and Chaos* **3**(1), 187–194.

Plenz, D. & Kitai, S. T. [1999] "A basal ganglia pacemaker formed by the subthalamic nucleus and external globus pallidus," *Nature* **400**, 677–682.

Rinzel, J. & Ermentrout, B. [1998] "Analysis of neural excitability and oscillations," in *Methods in Neuronal Modeling*, ed. Koch, C. & Segev, I. (The MIT Press, Cambridge), pp. 251–291.

Robinson, H. P. C., Kawahara, M., Jimbo, Y., Torimitsu, K., Kuroda, Y. & Kawana, A. [1993] "Periodic synchronized bursting and intracellular calcium transients elicited by low magnesium in cultured cortical neurons," *J. Neurosci.* **70**(4), 1606–1616.

Segundo, J. P., Stiber, M. & Vibert, J.-F. [1995] "Synaptic coding of spike trains," in *The Handbook of Brain Theory and Neural Networks*, ed. Arbib, M. A. (The MIT Press, Cambridge), pp. 953–956.

Selz, K. A. & Mandell, A. J. [1992] "Cortical coherence and characteristic times in brain stem neuronal discharge patterns," in *Single Neuron Computation*, ed.

McKenna, T., Davis, J. & Zornetzer, S. F. (Academic Press, Boston), pp. 525–560.

Szücs, A., Varona, P., Volkovskii, A. R., Abarbanel, H. D. I., Rabinovich, M. I. & Selverston, A. I. [2000] "Interacting biological and electronic neurons generate realistic oscillatory rhythms," *NeuroReport* **11**(3), 563–569.

Wang, X.-J. & Rinzel, J. [1995] "Oscillatory and bursting properties of neurons," in *The Handbook of Brain Theory and Neural Networks*, ed. Arbib, M. A. (The MIT Press, Cambridge), pp. 686–691.

Williams, T. L. & Sigvardt, K. A. [1995] "Spinal cord of lamprey: Generation of locomotor patterns," in *The Handbook of Brain Theory and Neural Networks*, ed. Arbib, M. A. (The MIT Press, Cambridge), pp. 918–921.

Yoshinaga, T., Kitajima, H., Kawakami, H. & Mira, C. [1997] "A method to calculate homoclinic points of a two-dimensional noninvertible map," *IEICE Trans. Fundamentals* **E80-A**(9), 1560–1566.

You, Z., Kostelich, E. J. & Yorke, J. A. [1991] "Calculating stable and unstable manifolds," *Int. J. Bifurcation and Chaos* **1**(3), 605–623.